JOURNAL OF MATERIALS SCIENCE 31 (1996) 4381–4385

Effects of cyclic stressing, heat treatment and shot-peening pressure on the residual stress distribution in two titanium alloys

B. R. SRIDHAR, K. RAMACHANDRA
Gas Turbine Research Establishment, Bangalore 560 093, India
K. A. PADMANABHAN
Department of Metallurgical Engineering, Indian Institute of Technology, Madras 600 036, India

Using the method of drilling holes, the residual stress distributions were determined in two titanium alloys, IMI-685 and IMI-318, in the machined, polished, shot-peened and cyclically stressed (MPSC) as well as the heat-treated and quenched (HTQ) conditions. In IMI-318, the effect of shot-peening pressure on the residual stress distribution was also studied. Tensile cyclic stressing relaxed the shot-peen induced residual stresses in the longitudinal direction and the extent of relaxation depended on the degree of cyclic softening present in the material. In both alloys, in the post-β heat-treated and quenched condition, the residual stresses were tensile in nature. In IMI-318, a decrease in the shot-peening pressure led to residual stresses of lower magnitudes. The peak residual stress was present closer to the surface when the shot-peening pressure was increased.

1. Introduction

Titanium alloys near-alpha IMI-685 (Ti–6Al–5Zr –0.5Mo–0.25Si, wt %) and the alpha–beta IMI-318 (Ti–6Al–4V, wt %) are used in gas turbine engines. The microstructures are, respectively, acicular α (HCP) in basket-weave form separated by thin layers of β (BCC) and equiaxed α with the β phase located at the α boundaries [1].

In an earlier paper, the residual stress distributions in these two alloys, estimated by the method of drilling holes, were reported for the machined, polished and shot-peened (MPS) condition (glass beads were used, pressure 480 kPa, intensity 35 N). In both the alloys, the residual stresses were compressive in nature. The peak longitudinal residual stress (− 710 MPa in IMI-685, and − 705 MPa in IMI-318) was present at the surface in the case of IMI-685, but it was observed in a sub-surface region in IMI-318 [1].

In this paper, the residual stress distributions in the above two alloys corresponding to some treatments not so far considered will be described.

2. Experimental procedures

From test rings of forgings of both alloys, specimens 75 mm × 15 mm × 5 mm in size were machined and polished down to 500 grade SiC emery. Glass beads of 0.1–0.2 mm diameter, suspended in water at a known concentration, were forced through a nozzle on to the polished specimen surfaces at a pressure of either 480 or 360 kPa for 2–3 min. The specimens were held between flat grips on an MTS servo-hydraulic machine and subjected to constant stress amplitude axial fatigue (R = minimum stress/maximum stress = 0) in a sinusoidal mode for about 5000 cycles (stress range 0–770 MPa; frequency 2 Hz).

Samples of size 25 mm × 15 mm × 10 mm were vacuum heat treated at 1050 °C for 30 min and quenched in argon by flushing with the gas (post-beta quenching). The specimens were cleaned using a dilute HF–HNO_3–water mixture to remove any oxidized layer that could be present.

The procedures for determining the residual stress distribution by the method of drilling holes have already been described [1]. For each increment in depth, readings from all three strain gauges in a standard strain-gauge rosette were noted. The strains relieved, ε_1, ε_2 and ε_3, were plotted as functions of dimensionless parameter, Z/D_0 (Z is the hole depth and D_0 is the hole diameter). Corresponding to different surface conditions, the principal residual stress components, σ_p and σ_q, as well as the longitudinal, σ_L, and transverse, σ_T, residual stress components, were evaluated. These were then presented as functions of depth below the surface.

3. Results and discussion

3.1. Residual stresses in IMI-685

3.1.1. Machined, polished, shot-peened and cyclically stressed (MPSC) condition

The shot-peening pressure was 480 kPa. The strains relieved following cyclic stressing are shown in Fig. 1 as functions of (Z/D_0). Compared to the machined,

0022–2461

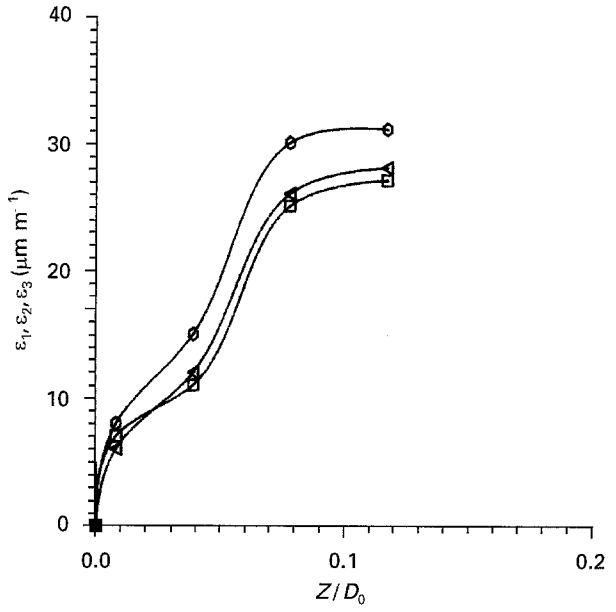

Figure 1 Variation of the strains relieved, (□) ε_1, (△) ε_2 and (⬡) ε_3, as functions of Z/D_0 in the machined, polished, shot-peened and cyclically stressed (0–770 MPa) condition. IMI-685; peening pressure 480 kPa.

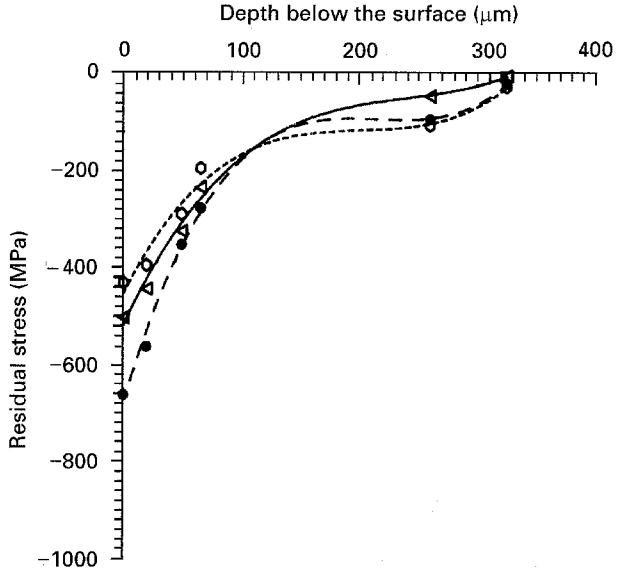

Figure 2 Variation of the principal residual stress components (—△—, σ_p; – –(⬡)– –, σ_q), and (– – ● – –) the longitudinal stress component (σ_L) as functions of depth in the machined, polished, shot-peened and cyclically stressed (0–770 MPa) condition. IMI-685; peening pressure 480 kPa.

polished and shot-peened (MPS) (also at 480 kPa) condition studied earlier [1], decreases in the magnitudes of the strains relieved were noted here. This indicated that the shot-peen induced strains were relaxed during cyclic stressing. In Fig. 2, a plot of σ_p and σ_q (both compressive) as functions of depth below the surface is presented. Compared with the MPS condition [1], σ_p here was less at all depths. σ_q showed a slight increase at the surface but was less in the sub-surface regions. The longitudinal stress, σ_L, also showed a trend similar to that of σ_p. The decrease in the surface was marginal ($\approx$50 MPa, $\approx$7%). However, the sub-surface stresses had decreased significantly. The residually stressed layer was also reduced in thickness by cyclic stressing (Fig. 2).

Residual stresses are known to relax on cyclic stressing [2–4]. (The presently applied tensile stress amplitude of 770 MPa, was well above the room-temperature endurance limit of 645 MPa for IMI-685.) The effective tensile cyclic stress amplitude is equal to the difference between the applied tensile (cyclic) stress amplitude and the magnitude of the compressive residual stress. As the peak longitudinal residual stress corresponding to the MPS condition was present in IMI-685 at the surface [1], the effective tensile cyclic stress amplitude was greater in the sub-surface regions than at the surface. This, in turn, led to greater localized strains and a larger relaxation of the residual stresses in the sub-surface regions compared to the specimen surface. This result is in contrast to that seen in tension–compression type of loading ($R = -1$) in which a larger relaxation of the residual stresses is present at the surface in comparison with the sub-surface regions [4, 5].

3.1.2. Heat-treated and quenched condition

Fig. 3 displays the strains relieved as functions of (Z/D_0) for a specimen given the heat treatment 1050 °C/0.5 h/argon quench. It is seen that the strains relieved were negative, and became increasingly so with depth.

The principal as well as the longitudinal and transverse residual stress components were tensile in nature and they decayed rapidly with depth (Fig. 4).

The magnitudes of the residual stresses were comparable to those found earlier by an X-ray method in IMI-685 cylinders quenched from 1050 °C [6]. In quenched steels, on the other hand, the residual stresses were compressive [7]. This difference in behaviour can be traced to the difference in the relative importance of the two processes: (a) volumetric expansion in the surface layers following martensite formation that gives rise to a residual compressive stress, and (b) greater thermal contraction of the surface layers due to quenching that gives rise to a residual tensile stress. (During quenching, surface layers cool faster compared to the core; as a result the surface layers contract more than the core. Because of the continuity of the medium the core resists the differential contraction

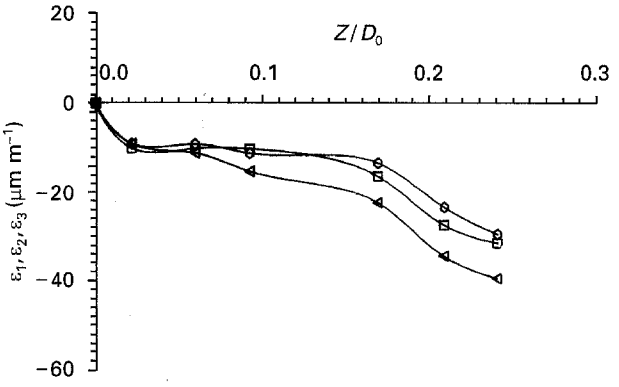

Figure 3 Variation of the strains relieved, (□) ε_1, (△) ε_2 and (⬡) ε_3, as functions of Z/D_0. IMI-685 subjected to the heat treatment at 1050 °C/0.5 h/argon quench.

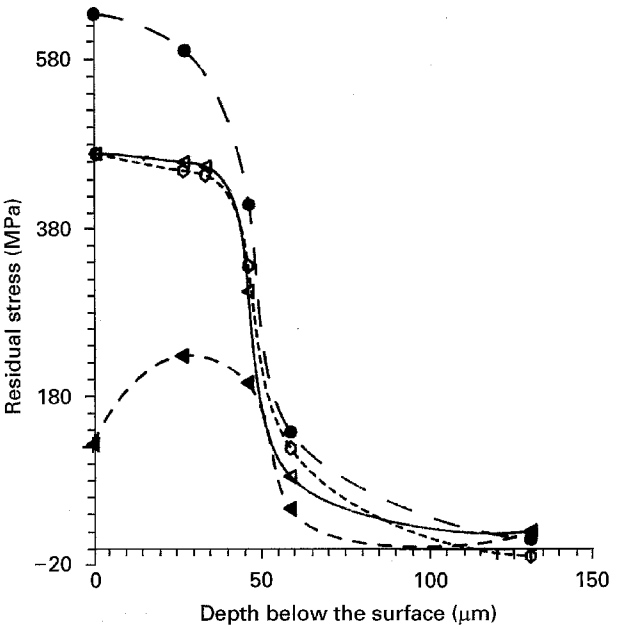

Figure 4 Variation of the principal (—△—, σ_p; --(○)--, σ_q), (—•—) longitudinal (σ_L) and (--◀--) transverse (σ_T) residual stress components as functions of depth. IMI-685 subjected to the heat treatment at 1050 °C/0.5 h/argon quench.

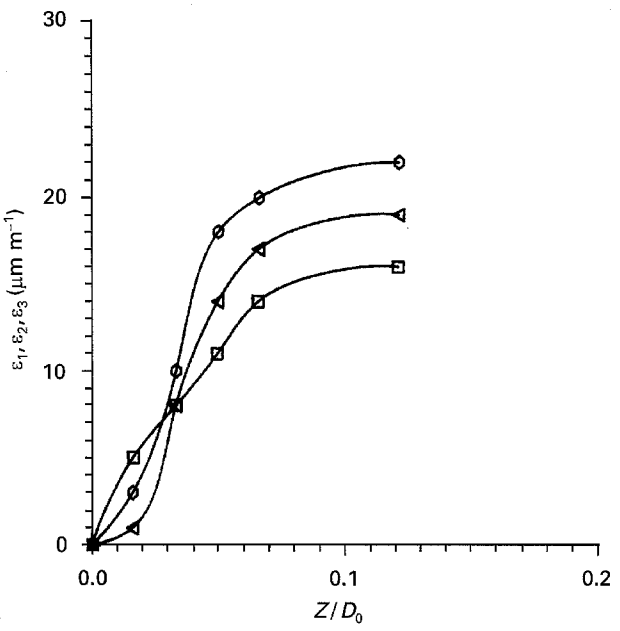

Figure 5 Variation of the strains relieved, (□) ε_1, (◁) ε_2 and (○) ε_3, as functions of Z/D_0. IMI-318; machined, polished and shot-peened condition, peening pressure 360 kPa.

of the surface layers, and this leads to the generation of tensile residual stress in the surface. To offset the tensile residual stress in the surface, compressive residual stress is generated in the core.) Evidently, in steels the former process is more dominant, but in IMI-685 the latter process seems to decide the nature of the residual stress. (See also discussion in Section 3.2.3.)

3.2. Residual stresses in IMI-318

3.2.1. Machined, polished and shot-peened (MPS) condition

In the earlier study [1], the shot-peening pressure was 480 kPa; here it was reduced to 360 kPa. Fig. 5 is a plot of the strains relieved as functions of (Z/D_0) and it is clear that the variation was similar to that discussed above. However, the strains relieved were less than when the peening pressure was 480 kPa [1]. This is indicative of a direct dependence between the degree of cold work and the peening pressure.

The principal, longitudinal and transverse residual stresses are displayed in Fig. 6 as functions of depth below the surface. As in the earlier study [1], they were all compressive in nature but the magnitudes here were less due to the lower peening pressure. Also, the residually stressed layer was only 250 μm deep in comparison with a depth of 800 μm in the previous study.

The peak principal residual stress component, σ_p, for a peening pressure of 480 kPa was − 544 MPa [1]. This works out to 58% of the room-temperature 0.2% proof stress of IMI-318 (930 MPa). The corresponding ratio for the present experiments, where the peening pressure was 360 kPA, is 41%. Thus, an earlier conclusion [8], that in this alloy the residual stress peak is about 50%–60% of the yield strength of the material, cannot be regarded as always valid, as the peening pressure also appears to affect the ratio of the peak residual stress to the 0.2% yield strength.

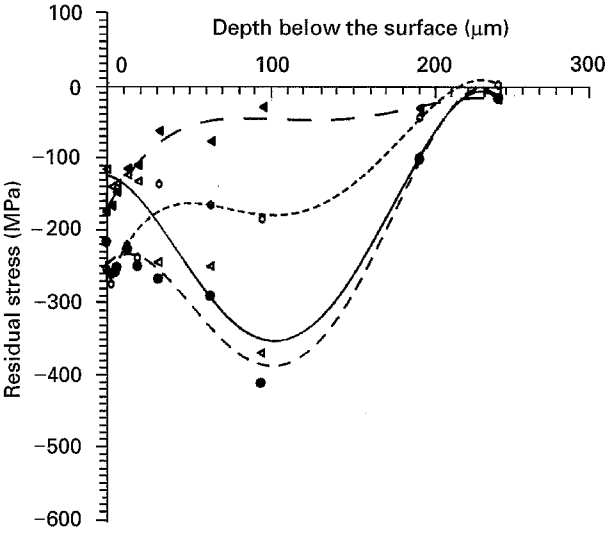

Figure 6 Variation of the principal (—◁—, σ_p; --(○)--, σ_q), (—•—) longitudinal (σ_L) and (--◀--) transverse (σ_T) residual stress components as functions of depth below the surface. IMI-318; machined, polished and shot-peened condition, peening pressure 360 kPa.

The lower thickness of the residually stressed layer in the present case is directly traceable to the lower energy supplied during shot peening compared with the earlier case [1].

In the previous study [1], the peak residual stress was found at a depth of 25 μm below the surface. Here, it is seen that at a depth of 100 μm (Fig. 6). The observed shift is in line with an earlier finding [9] that the peak residual stress moves towards the surface with increasing degree of cold work/peening pressure.

3.2.2. Machined, polished, shot-peened and cyclically stressed (MPSC) condition

The shot-peening pressure was 360 kPa and the cyclic stress range 0–770 MPa. Fig. 7 is a plot of the strains

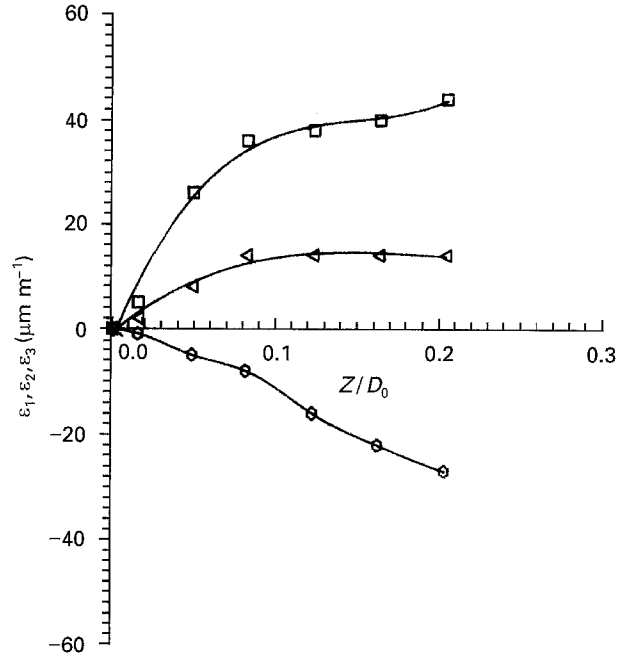

Figure 7 Variation of the strains relieved, (□) ε_1, (◁) ε_2 and (⬡) ε_3, as functions of Z/D_0. IMI-381; machined, polished, shot-peened and cyclically stressed (0–770 MPa) condition, peening pressure 360 kPa.

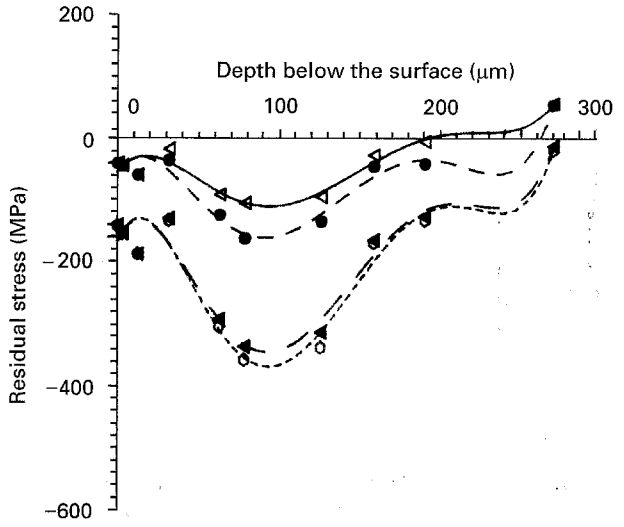

Figure 8 Variation of the principal (—◁—, σ_p; ——(⬡)——, σ_q), (– –●– –) longitudinal (σ_L) and (– –◀– –) transverse (σ_T) residual stress components as functions of depth below the surface. IMI-318; machined, polished, shot peened and cyclically stressed (0–770 MPa) condition, peening pressure 360 kPa.

relieved for the MPSC condition. The extent of relaxation here was significantly greater than that for IMI-685. It is also seen from Fig. 8 that, compared with the unstressed condition (Fig. 6), σ_p had diminished but σ_q had increased. There was no change in the depth of the residually stressed layer. The pattern of distribution of the longitudinal and transverse components was similar to those of the principal stress components.

A negative ε_3 (Fig. 7) in a direction that coincided with the axis of the tensile cyclic stresses indicated that tensile cyclic stressing relieved the original residual compressive strains (positive) to zero and, in addition,

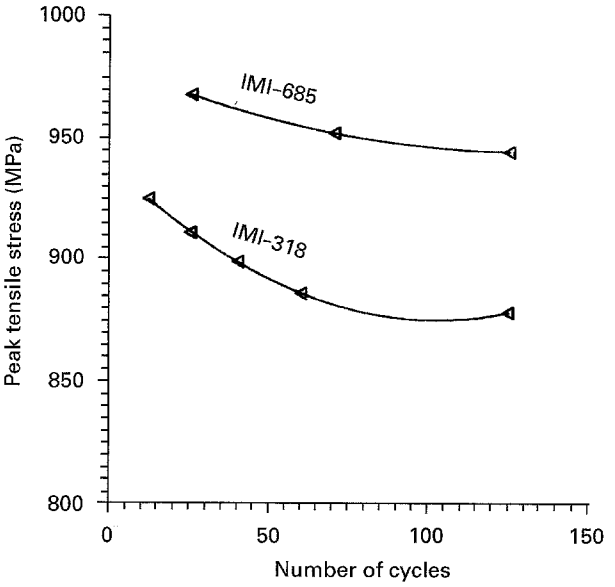

Figure 9 Cyclic softening in IMI-685 and IMI-318 during room-temperature low-cycle fatigue deformation (strain amplitude ± 1.1%, strain rate 3×10^{-3} s^{-1}).

caused an expansion of surface layers (and so during the drilling of a hole, negative ε_3 values were obtained). Tensile cyclic stresses in the longitudinal direction cause cyclic compression in the transverse direction which were added to the already existing compressive strains. Therefore, the residual stresses and the strains released in the transverse direction (ε_1) were quite substantial.

In microstructures exhibiting cyclic hardening or slight softening, the decay of the residual stresses is much less than in materials undergoing large cyclic softening [10]. IMI-318 undergoes large cyclic softening in fatigue, but cyclic softening in IMI-685 is only marginal (Fig. 9) (see also Wagner and Luetjering [10, 11]). Therefore, the residual stress relaxation following cyclic stressing in IMI-318 was to the tune of 60% of the peak longitudinal residual stress while in IMI-685 shot peened at 480 kPA, the residual stress relaxation on cyclic stressing was only of the order of 10%.

3.2.3. Heat-treated and quenched condition

The strains relieved on drilling a hole in post-beta quenched IMI-318 samples (Fig. 10) were similar to those reported for IMI-685 (Fig. 3). The principal, as well as the longitudinal, residual stress components were tensile in nature (Fig. 11). To a depth of about 80 μm, both σ_p and σ_q had magnitudes greater than 150 MPa.

In an earlier study [12] the improvement in fatigue life following β quenching was attributed to the surface compressive stresses generated by hexagonal martensite (α′) formation. A selected-area diffraction analysis of the present sample [13] indicated only the presence of α, which forms by a nucleation and growth process and apparently does not cause, during quenching, much differential expansion at the surface layers. Water/brine quenching might have led to the formation of α′ [14, 15].

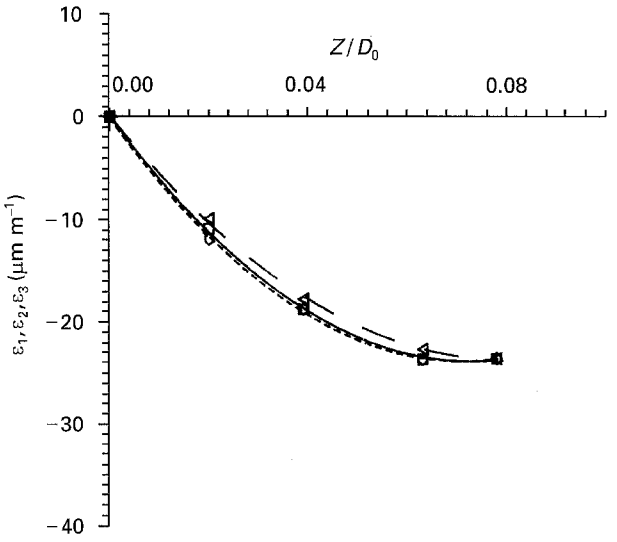

Figure 10 Variation of the strains relieved, (—□—) ε_1, (—◁—) ε_2 and (—(◯)—) ε_3, as functions of Z/D_0. IMI-318 subjected to the heat treatment at 1050 °C/0.5 h/argon quench.

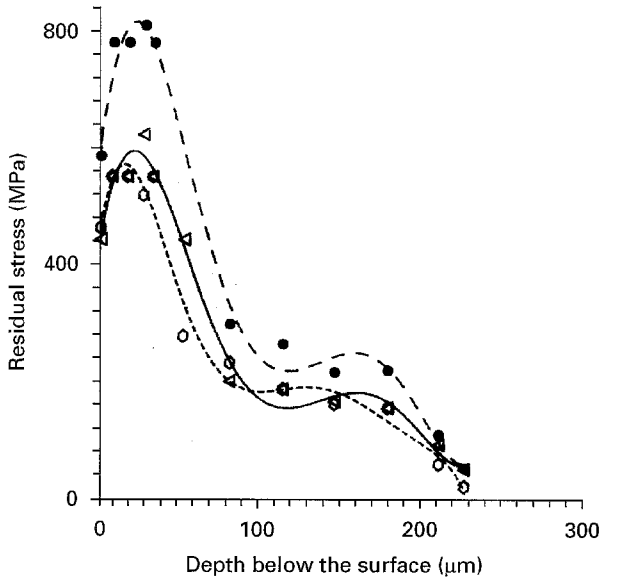

Figure 11 Variation of the principal (—△—, σ_p; --(◯)--, σ_q), and (--●--) longitudinal (σ_L) residual stress components as functions of depth below the surface. IMI-318 subjected to the heat treatment at: 1050 °C/0.5 h/argon quench.

Evidently, the results presented in Section 3 have implications for the fatigue behaviour of the two alloys, IMI-685 and IMI-318.

4. Conclusions

The following conclusions have emerged from the present study on two titanium alloys, IMI-685 and IMI-318.

1. In both the alloys, cyclic tensile stressing ($R = 0$) led to a relaxation of shot-peen induced residual stresses.

2. In both materials, the sub-surface stresses relaxed far more than the surface residual stresses. The behaviour was contrary to that reported in an earlier study involving compression–tension type of loading.

3. In IMI-318 the magnitudes of the residual stresses decreased with decreasing peening pressure. Also, the peak residual stress was present closer to the specimen surface on increasing the peening pressure.

4. The extent of relaxation on tensile cyclic stressing was greater in IMI-318 than in IMI-685, presumably because of the larger cyclic softening present in IMI-318 (compared with IMI-685).

5. In both alloys, post-beta quenching gave rise to tensile residual stresses.

Acknowledgements

The authors thank Dr R. Krishnan, Director, Gas Turbine Research Establishment, Bangalore, for encouragement. K. A. Padmanabhan thanks the Alexander von Humboldt – Stiftung, Bonn, for a stay in Germany on a "Forschungspreis" that enabled him to finalize this paper.

References

1. B. R. SRIDHAR, W. G. NAFDE and K. A. PADMANABHAN, *J. Mater. Sci.* **27** (1992) 5783.
2. M. DESVIGNES, B. GENTIL and L. CASTEX, in "Second International Conference on Impact Treatment Processes", edited by S. A. Meguid (Elsevier Applied Science, London, New York, 1986) pp. 250–7.
3. J. BERGSTROM, in "Advances in Surface Treatment Technology, Applications and Effects", Vol. 3 (Pergamon, Oxford, 1986) pp. 97–112. Cited in *Met. Abs* 31-4159, Sept. 1987, Vol. 20, p. 73.
4. J. BERGSTROM and T. ERICSON, *Surf. Eng.* **2** (1986) 115.
5. O. VOHRINGER, in "Advances in Surface Treatment Technology, Applications and Effects", Vol. 4 (Pergamon, Oxford, 1986), pp. 367–96. Cited in *Met. Abs.* 31-4173, Sept. 1987, Vol. 20, p. 74.
6. S. DENNIS, J. C. CHEVERIER and G. BECK, in "Titanium Science and Technology (1980)", Vol. 2, Proceedings of the Fourth International Conference of Titanium, edited by H. Kimura and O. Izumi (Metallurgical Society of AIME, Warrendale, PA, 1980) pp. 1563–69.
7. A. NICKU-LARI, J. KU and J. F. FLAVENOT, *Exp. Mech.* **25** (1985) 175.
8. J. D. ALMEN and P. H. BLACK, "Residual Stresses and Fatigue in Metals" (McGraw Hill, New York, 1963) pp. 65–90.
9. H. WOHLFAHRT, in "Proceedings of the Second International Conference on Shot Peening (ICSP-1)", edited by H. O. Fuchs (American Shot Peening Society, Paramus, NJ, 1984) pp. 306–15.
10. L. WAGNER and G. LUETJERING, *ibid.*, pp. 194–200.
11. *Idem, ibid.*, pp. 201–7.
12. J. C. WILLIAMS, A. W. THOMPSON, C. G. RHODES and J. C. CHESSNUT, in "Titanium and Titanium Alloys", Vol. 1, Proceedings of the Third International Conference on Titanium, edited by J. C. Williams and A. F. Belov (Plenum, New York, 1982) p. 467.
13. B. R. SRIDHAR, PhD thesis, Indian Institute of Technology, Madras (1994).
14. P. RAMA RAO, personal communication, dated 10 July 1992.
15. E. W. COLLINGS, "The Physical Metallurgy of Titanium Alloys" (American Society for Metals, Metal Park, OH, 1984).

Received 12 January 1995
and accepted 13 February 1996